MODELING SPATIAL PATTERNS IN FISHERIES BYCATCH: IMPROVING BYCATCH MAPS TO AID FISHERIES MANAGEMENT

Michelle Sims,[1,3] Tara Cox,[1] and Rebecca Lewison[2]

[1]*Center for Marine Conservation, Nicholas School of the Environment and Earth Sciences, Duke University Marine Lab,*
135 Duke Marine Lab Road, Beaufort, North Carolina 28516 USA
[2]*San Diego State University, Biology Department, 5500 Campanile Drive, San Diego, California 92182-4614 USA*

Abstract. Fisheries bycatch, or incidental take, of large vertebrates such as sea turtles, seabirds, and marine mammals, is a pressing conservation and fisheries management issue. Identifying spatial patterns of bycatch is an important element in managing and mitigating bycatch occurrences. Because bycatch of these taxa involves rare events and fishing effort is highly variable in space and time, maps of raw bycatch rates (the ratio of bycatch to fishing effort) can be misleading. Here we show how mapping bycatch can be enhanced through the use of Bayesian hierarchical spatial models. We compare model-based estimates of bycatch rates to raw rates. The model-based estimates were more precise and fit the data well. Using these results, we demonstrate the utility of this approach for providing information to managers on bycatch probabilities and cross-taxa bycatch comparisons. To illustrate this approach, we present an analysis of bycatch data from the U.S. gill net fishery for groundfish in the northwest Atlantic. The goals of this analysis are to produce more reliable estimates of bycatch rates, assess similarity of spatial patterns between taxa, and identify areas of elevated risk of bycatch.

Key words: Bayesian spatial models; bycatch; conditional autoregressive prior; fisheries mapping; marine mammals; Markov chain Monte Carlo (MCMC); seabirds; sea turtles; spatial statistics.

INTRODUCTION

Fisheries bycatch, or incidental take, is a pressing conservation and fisheries management issue worldwide (Kelleher 2005). There is particular concern regarding bycatch of large pelagic and coastal vertebrates (Lewison et al. 2004). Given the efforts to mitigate and minimize bycatch of these vulnerable species, maps of bycatch events have a variety of uses. They are a powerful exploratory tool that can be used to describe the spatial variation in bycatch; in particular they may identify bycatch "hotspots" for particular taxa. In addition, bycatch maps can help site and then fine tune the location and extent of management areas. For example, the temporary closure of a given area, referred to as a time-area closure, has been used in numerous fisheries to reduce the amount of bycatch of protected species. Examples include harbor porpoises in the Gulf of Maine (U.S. Department of Commerce 1998), sea turtles in the California drift net fishery (Caretta et al. 2005), and seabirds in the Southern Ocean (Croxall and Nicol 2004). Finally, bycatch maps can also be compared to the spatial distribution of environmental factors (e.g., sea surface temperature, currents, or eddies) to improve our understanding of the oceanographic context of animal distribution and subsequent

fisheries bycatch (Polovina et al. 2004, 2006, James et al. 2005).

There are several inherent features of bycatch data on large vertebrates that make mapping these data challenging. Bycatch is a rare event, but although the majority of counts will be zero there may also be large counts resulting from aggregations of animals. This typically results in a distribution that is overdispersed relative to the Poisson assumption. Another feature is the spatial resolution of the data, particularly in how the bycatch event is geographically referenced. Bycatch data may be georeferenced by the point location of the fishing haul or set, but often a bycatch event may be referenced by a spatial area such as a grid cell. A further challenging feature concerns the distribution of fishing effort. Because the goal of a fishery is to target particular fish species, fishing effort is nonrandomly distributed. Since the number of bycatch events is expected to be positively correlated to the effort expended in a particular area, a simple map showing the number of bycatch events without accounting for this spatial variation in effort will be misleading. It is more appropriate to construct maps of bycatch rates, which are the ratio of bycatch to fishing effort.

Given the challenges of modeling and mapping bycatch data, we present an approach that quantifies the amount of true spatial variation in bycatch rates between grid cells. A map of raw bycatch rates can misrepresent the true spatial distribution of bycatch rates. For example, suppose a region is divided into N

contiguous areas, $i = 1, \ldots, N$. If O_i represents the observed bycatch in area i and E_i represents the observed fishing effort in area i, then the raw bycatch rate R_i, also the maximum likelihood estimate under Poisson assumptions on O_i, is computed as

$$R_i = \frac{O_i}{E_i} \qquad (1)$$

with a standard error given by

$$\mathrm{SE}(R_i) = \frac{\sqrt{O_i}}{E_i} \qquad (2)$$

(Leyland and Davies 2005).

When observed fishing effort in an area is low, a small change to the number of observed bycatch events will result in a large change to the raw rate. This may give rise to unusually high or low rates in areas of low effort. This illustrates the central problem with raw rates: some areas may appear to have higher bycatch rates only because they have low observed fishing effort. Accordingly, the variability of the raw rate is inversely proportional to fishing effort (Eq. 2). Thus, given an equal number of observed bycatch events, the standard error for a rate estimated with low effort will be larger compared to a rate estimated with high effort. An additional problem of using raw rates surrounds the treatment of zeros. If the observed bycatch in an area was zero then the standard error is also zero, but this does not allow for any random variation in the expected count.

Here we present a case study in which we illustrate a model-based approach for the construction of bycatch maps to estimate the distribution of true bycatch rates while accounting for rarity of bycatch and differences in effort among areas. We demonstrate the utility of this approach using marine mammal and seabird bycatch data collected from the U.S. gill net fishery for groundfish in the northwest Atlantic, which operates from the U.S.–Canada border in the north to the North Carolina–South Carolina border in the south. The approach presented uses a spatial model developed for epidemiology and public health (Besag et al. 1991, Cressie et al. 2000, Best et al. 2005) that can separate the variability in true bycatch rates from random variation: something that is not possible with maps of raw rates. The model uses data from neighboring areas to gain precision in an estimated rate for a particular area (or grid cell) by an amount that depends on its observed fishing effort. Areas with low fishing effort make more use of the data from surrounding areas to gain precision. The result is a spatial map of smoothed bycatch rates, with greater stability in estimates for individual areas, allowing more confidence to be placed in their interpretation.

Using these data, we first model the bycatch rates of marine mammals and seabirds using Bayesian hierarchical spatial models. We then illustrate two novel applications of this approach: mapping the probability that bycatch exceeds a specified threshold rate of interest and identifying areas of high multispecies or taxa bycatch. A map of exceedence probabilities identifies areas in which bycatch rates are likely to be above a particular threshold, a risk level that can be set to reflect the population status of a particular species of management or conservation concern. The multitaxa application considers how the spatial distribution of bycatch rates varies among taxa. Typically, bycatch is evaluated for a single species. However, cross-taxa analyses provide a broader perspective on spatial patterns of bycatch by considering bycatch patterns across taxa and can facilitate management efficiency in identifying zones (e.g., time-area closure candidates) based on a more comprehensive understanding of the ecological impacts of a particular fishery.

METHODS

Data

Data used in the analyses were collected by National Marine Fisheries Service, Northeast Fisheries Science Center (NMFS, NEFSC) observers onboard vessels of the U.S. gill net fleet (NMFS Northeast Fisheries Observer Program, *unpublished data*) (see Plate 1). Observers are placed on a random sample of fishing vessels and record location of the net, target species, number of nets in the string, mesh size, soak duration, depth at which the net was set, presence or absence of pingers, and bycatch per haul. Due to confidentiality agreements, the spatial information for each haul was aggregated to $0.5° \times 0.5°$ square grid cells.

There were 65 712 hauls from 1440 trips from 1990 to 2004. In order to increase our sample size, we had to collate data either across years or across seasons. We expected that there would be relatively little interannual variability in animal movements within a season (see Read and Westgate 1997). In addition, management tools, especially time-area closures, can be seasonal, but need to be consistent across years. Thus, we collated data across years. Marine mammals and seabirds in this region have known seasonal movement (Read and Westgate 1997, Ronconi 2007), so we split the data into four seasons: Season 1 (January–March), Season 2 (April–June), Season 3 (July–September), and Season 4 (October–December). In each season, we used the total number of bycatch events and total fishing effort from all hauls observed in a grid cell to construct the model. Hauls were observed in 83, 112, 87, and 93 grid cells during Seasons 1–4, respectively. After removing isolated groups of grid cells (one or more grid cells defines a group) for which there were no observed bycatch events in any cell (requirement of the model fit), this was reduced to 82, 102, 54, and 82 grid cells for each season, respectively. Since fishing effort in Season 3 was restricted to a much smaller spatial region compared with the other three seasons, we excluded Season 3 from the analyses.

PLATE 1. Retrieving a gillnet from the water. Photo credit: Chris Doley, courtesy of the National Oceanic and Atmospheric Administration Restoration Center.

We used net length (meters) multiplied by soak time (hours) as a measure of fishing effort. We also could have used the number of hauls as a unit of effort. However, the correlation between total hauls and total net length by soak time per grid cell was high ($r = 0.879$, 0.941, and 0.95 for Seasons 1, 2, and 4, respectively; $P < 0.001$) so we are confident that using total hauls would not have changed the results significantly. Bycatch rates are presented in the results as the number of individuals caught per 1000 units of effort.

MODELS

Single-taxon analysis

The methodology for smoothing spatial data is widely accepted as a method in mapping of diseases in epidemiology and public health (e.g., see Besag et al. 1991, Knorr-Held and Besag 1998, Cressie et al. 2000, Dongchu et al. 2000, MacNab and Dean 2002, Best et al. 2005). Here, we adopt a similar approach proposed by Besag et al. (1991) and smooth raw rates using a Bayesian hierarchical spatial model of the form

$$O_i \sim \text{Poisson}(E_i R_i)$$
$$\log(R_i) = \alpha + S_i + U_i \quad (3)$$

where α is the average log bycatch rate across the whole region and S_i and U_i are random effects capturing the deviation of the expected bycatch rates in area i from the regional average. The random effects can be thought of as representing the effect of unobserved factors that have increased the variability in bycatch rates beyond that expected by the Poisson distribution alone: S_i represents the effects of unknown covariates that are spatially correlated, while U_i represents the effects of spatially unstructured covariates. The Besag model has the advantage of flexibility; it allows for both spatially structured correlation and unstructured overdispersion

in bycatch rates using random effects S_i and U_i, respectively, but lets the data decide how to partition the extra-Poisson variability between the two random effects.

We fit Model 3 to the aggregated marine mammal bycatch data. A conditional autoregressive (CAR) prior was assigned to the spatial effects S_i and a normal prior to the nonspatial effects U_i. Thus,

$$S_i | S_j, i \neq j \sim \mathcal{N}\left(\bar{s}, \frac{\sigma_s^2}{k}\right)$$
$$U_i \sim \mathcal{N}(0, \sigma_u^2)$$

where S_j are all areas excluding the ith area, $\bar{s}$ is the average of the random effects S_j that are neighboring areas of S_i, and k is the number of neighbors. The spatial random effects S_i are smoothed towards the mean of the spatial random effects in neighboring areas, to account for the spatial dependence, by an amount that depends on the effort in that area and its number of neighbors k. We define a set of neighbors for grid cell i as all grid cells that share a common boundary to grid cell i.

Cross-taxa analysis

The model for the cross-taxa analysis is of the form

$$O_{1i} \sim \text{Poisson}(E_i R_{1i})$$
$$O_{2i} \sim \text{Poisson}(E_i R_{2i})$$
$$\log(R_{1i}) = \alpha_1 + S_{1i} + U_{1i} \quad (4)$$
$$\log(R_{2i}) = \alpha_2 + S_{2i} + U_{2i}$$

where O_{1i} is the observed marine mammal bycatch and O_{2i} is the observed seabird bycatch in grid cell i. The subscripts 1 and 2 identify the terms in Model 4 for marine mammals and seabirds, respectively. We assumed independent normal priors with mean zero and variances σ_{1u}^2 and σ_{2u}^2 for U_{1i} and U_{2i}, respectively. The

model assumes that for each taxon the bycatch rates are spatially correlated and that within an area bycatch rates are correlated among taxa. These assumptions are represented by the intrinsic bivariate normal CAR prior (Thomas et al. 2004). This gives the distribution of S_{1i} and S_{2i} as

$$\frac{S_{1i}}{S_{2i}} \Bigg| \frac{S_{1j}}{S_j} \, i \neq j \sim \mathcal{N}\left(\begin{bmatrix} \bar{s}_1 \\ \bar{s}_2 \end{bmatrix}, \begin{bmatrix} \dfrac{\sigma_{1s}^2}{k} & \dfrac{\sigma_{12s}}{k} \\ \dfrac{\sigma_{12s}}{k} & \dfrac{\sigma_{2s}^2}{k} \end{bmatrix} \right) \quad (5)$$

where $\bar{s}_1$ and $\bar{s}_2$ are the averages of all spatial random effects that are neighboring areas of S_{1i} and S_{2i}, respectively, σ_{1s}^2 and σ_{2s}^2 are their conditional variances, and σ_{12s} is the conditional covariance between S_1 and S_2 within a grid cell.

The main focus of this cross-taxa analysis is to calculate the within grid cell conditional correlation between the spatial components S_{1i} and S_{2i}:

$$\rho = \frac{\sigma_{12s}}{\sqrt{\sigma_{1s}^2 \sigma_{2s}^2}}.$$

Values for ρ close to one indicate a strong positive correlation between the bycatch rates of marine mammals and seabirds across all cells. This would suggest that the spatial patterns of their bycatch rates are similar due to shared spatially correlated covariates.

The single-taxon and cross-taxa analyses for each season were performed using Markov chain Monte Carlo (MCMC) simulations in WinBUGS 1.4 (Spiegelhalter et al. 2003). We specified noninformative independent priors for parameters in the model. As a requirement of fitting this type of model in WinBUGS, the mean rates (α, α_1, α_2) were given improper uniform priors on the whole real line. Based upon suggestions by Gelman (2006), the standard deviation parameters σ_u, σ_s, σ_{1u}, and σ_{2u} were given uniform distributions on the interval [0, 100]. The precision parameter (inverse variance) of the intrinsic bivariate normal CAR prior was given a Wishart ($\mathbf{R}$, p) distribution. To represent vague prior knowledge about the precision, we set $\mathbf{R}$ equal to a 2×2 identity matrix and p equal to 2 (Spiegelhalter et al. 1996). We monitored convergence by simulating three independent runs with widely dispersed initial values. We assumed the runs had converged when the means and 95% credible intervals of each run were similar to runs combined (Brooks and Gelman 1998). Convergence was achieved after 10 000 iterations and results are based on the next 200 000 iterations from one chain, keeping one in every 10 iterations to reduce autocorrelation in the samples.

In a Bayesian analysis a posterior distribution is obtained for the bycatch rate in each grid cell, describing how probable different bycatch rates are, given the observed bycatch. Results of the fitted models are presented as maps of the estimated posterior median

bycatch rates. Mapping the mean or median posterior value does not fully exploit the posterior distribution that is obtained for the bycatch rate in each grid cell. Therefore, we also consider posterior probabilities that the estimated area-specific bycatch rate $\hat{R}_i$ exceeds a specified threshold of interest. We set the threshold level at 0.0005 for illustration purposes only. To investigate the relative contribution of the unstructured and spatially structured components to the extra-Poisson variation, we calculated the quantity $\psi = \text{var}_s / (\text{var}_s + \sigma_u^2)$ (Thogmartin et al. 2004), where var_s is the marginal variance of the spatial component. We approximate the posterior distribution of the marginal variance using the empirical variance of the spatial random effects.

Results

The aggregated bycatch data are typical of overdispersed data. The distribution of counts of marine mammals encountered during Seasons 1, 2, and 4 (after data reduction) was highly skewed to the right, with 62% of the grid cells having zero bycatch (Fig. 1a). Fig. 1b gives a comparison of the raw marine mammal bycatch rates with the fishing effort for grid cells from Season 1. Grid cells with low fishing effort had the highest raw rates, illustrating the tendency for areas of low fishing effort to be associated with extremely high or low raw bycatch rates.

Single-taxon analysis

Model selection.—We considered whether a spatial component was necessary in the model by looking at the strength of spatial autocorrelation in random effects U_i estimated from Model 3 fit with no spatial effects S_i. Moran's I was calculated for distance classes of width 60 km (distances measured at centroids of grid squares), and Monte Carlo permutation procedures were used with 1000 permutations to test the significance of the autocorrelation for each distance class. Estimates of U_i showed evidence of spatial dependence. The spatial correlograms of the U_i's for Seasons 1, 2, and 4 are displayed in Fig. 2. In all seasons, there was significant positive correlation in bycatch rates observed up to 60 km apart. As distances between the centroids of neighboring grid squares are <60 km, a model with only nonspatial effects is evidently inappropriate.

Model 3, with spatial and nonspatial random effects, was compared to a model with only spatial effects using the deviance information criterion (DIC; Spiegelhalter et al. 2002). The DIC is the Bayesian model selection tool; the preferred, most parsimonious model is one with the lowest DIC. The difference in DIC between competing models and the one with lowest DIC (ΔDIC) must be greater than two for the support to lie solely with the latter (Spiegelhalter et al. 2002). Values of the DIC are given in Table 1. With the exception of Season 4, the model with spatial and nonspatial effects was the favored model (ΔDIC > 2). Both models deserved similar support in Season 4 (ΔDIC = 0.373). However,

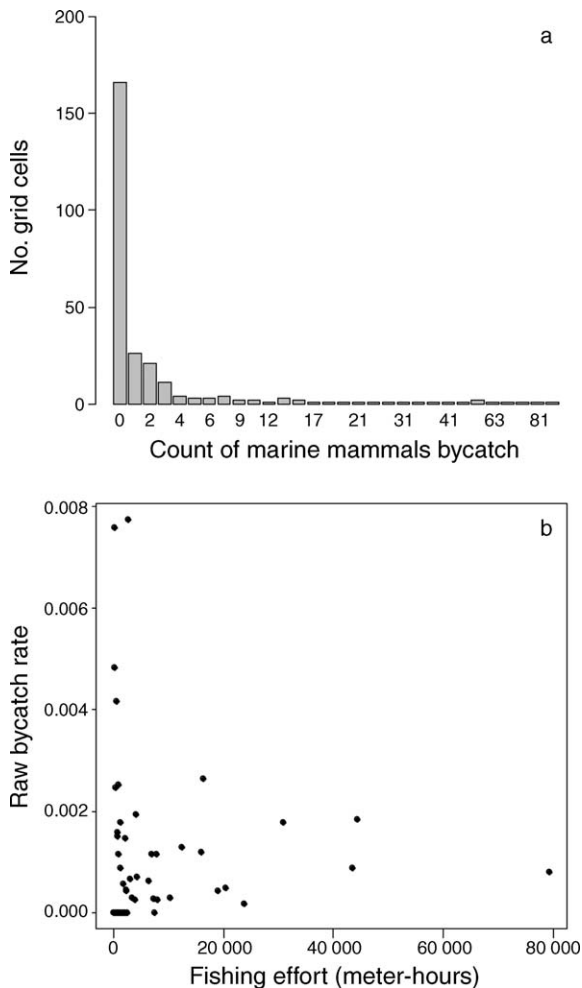FIG. 1. Data used in analysis. (a) Distribution of marine mammal bycatch in 0.5° × 0.5° square grid cells from 1990 to 2004 for all seasons combined. (b) Comparison of raw bycatch rate and fishing effort in each grid cell using data collected in Season 1. Raw bycatch rate = ratio of observed bycatch to fishing effort; fishing effort = net length (meters) multiplied by soak time (hours). Only Season 1 is shown for illustration purposes; Seasons 2 and 4 showed similar patterns.

we present results from fitting the simpler model, with only a spatial random effect, to marine mammal bycatch. Similarly, we drop the nonspatial random effect U_{1i} from the marine mammal component of the cross-taxa model when fit to Season 4 data. The relative contributions of the spatial and nonspatial components to the extra-Poisson variation in Model 3 gave further support to the final models selected. Approximately 31%, 58%, and 85% of the extra-Poisson variation was attributable to unknown spatially correlated covariates in Seasons 1, 2, and 4, respectively (Table 1).

Goodness-of-fit of the most parsimonious model for each season was assessed using Bayesian P values (Gelman et al. 1996, Morgan 2000). We used the deviance as the goodness of fit criteria. At each iteration

of the Markov chain Monte Carlo (MCMC), we calculated the deviance of the observed data (D) and the deviance of data simulated from the model given the current parameter values (D^*). The Bayesian P value measures the proportion of times D^* is greater than D. If the model fits the observed data well, then there should be little difference between fits of the observed and simulated data and the P value should be around 0.5. The magnitude of the P values obtained from the most parsimonious model for each season were all close to 0.5, suggesting that they fit the data well (Table 1).

Maps.—Smoothing of the grid cell bycatch rates by the best fitting spatial model is illustrated in Fig. 3 for Season 1. The amount of smoothing is related to fishing effort; grid cells with low fishing effort typically had the most smoothing, while estimates in cells of high fishing effort remained similar to their corresponding raw rates.
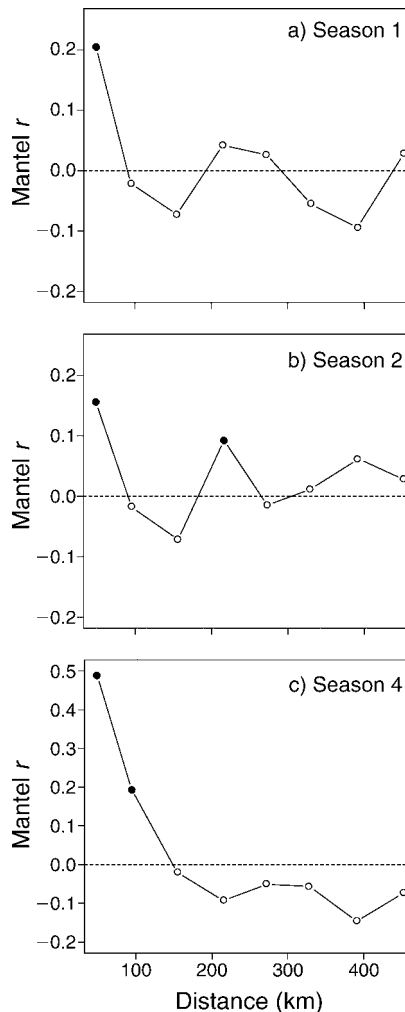

FIG. 2. Mantel correlogram of predicted random effects U_i from a single-taxon model with no spatial random effects for (a) Season 1, (b) Season 2, and (c) Season 4. Solid circles represent autocorrelation coefficients that are significantly different from zero.

TABLE 1. Summary statistics of the single-taxon and cross-taxa models.

	Single-taxon model				Cross-taxa model	
Season	Random effects	ψ	Bayesian P value	DIC	$P(\hat{\rho} > 0)$	Median estimate of $\hat{\rho}$ (95% CI)
1	S			227.097		
	S + U	0.31	0.529	218.085	0.726	0.384 (−0.709, 0.893)
2	S			245.530		
	S + U	0.58	0.531	242.507	0.368	−0.210 (−0.864, 0.785)
3	S		0.509	161.674	0.823	0.390 (−0.416, 0.900)
	S + U	0.85		162.047		

Notes: Shown for each season are the single-taxon models fit and their corresponding deviance information criterion (DIC), ψ for the models with both spatial and nonspatial random effects [$\psi = \text{var}_s/(\text{var}_s + \sigma_u^2)$], and a Bayesian P value for the best-fitting models (shown in bold). Estimates of the conditional correlation between seabird and marine mammal bycatch rates in a grid cell ($\hat{\rho}$) estimated by the cross-taxa model are also given (posterior median with 95% credible interval and the probability that $\hat{\rho}$ is greater than zero). Season 3 was excluded from the analysis because fishing effort in Season 3 was restricted to a much smaller spatial region. S = spatial random effect, U = nonspatial random effect.

The standard error of the model-estimated rates was generally lower than the raw rate standard error in a grid cell (Fig. 4), illustrating the reduction in variance that is achieved by smoothing bycatch rate estimates. This was most pronounced in grid cells with large raw rate standard errors (i.e., in those cells with low effort). Grid cells with a raw rate of zero were excluded from Fig. 4 since the corresponding standard error of zero would not necessarily be representative of the random variation in the rate.

Figs. 5a, b, 6a, b, and 7a, b show the raw rates and smoothed rates estimated by the best fit model for Seasons 1, 2, and 4, respectively. There were more areas with high bycatch rates (>0.0004) in Seasons 1 and 2 than in Season 4. The highest rates appear to be in the northern and southern regions in Season 1 and the northern region for Season 2. Bycatch rates for Season 4 were highly localized in these areas. The differences in magnitude between the standard errors of the raw and smoothed rates are shown in Figs. 5c, 6c, and 7c for Seasons 1, 2, and 4, respectively. Grid cells with a raw rate of zero were excluded from the comparison for reasons outlined in the paragraph above. The standard errors associated with the smoothed rates were generally smaller than the standard errors of the raw rates, with the difference in magnitude as large as 0.005 for Season
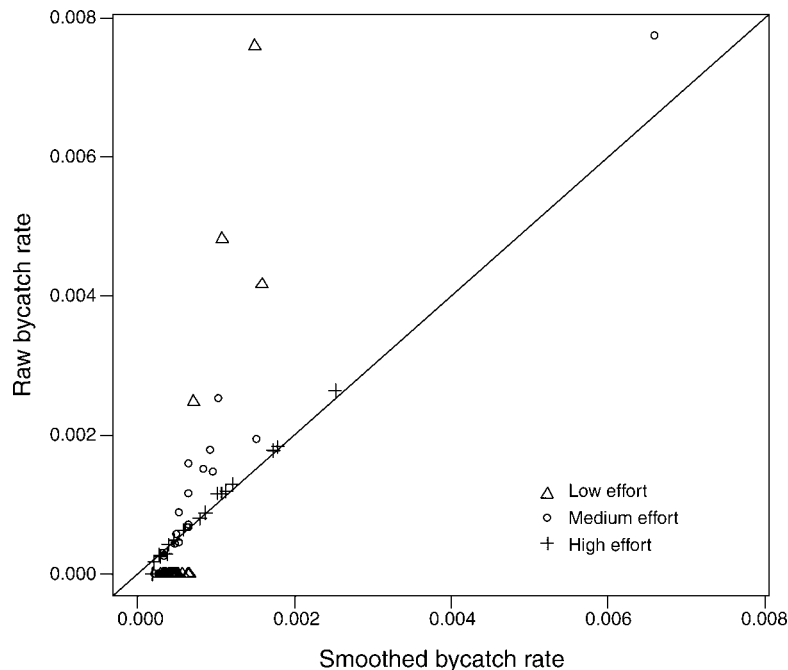

FIG. 3. Comparison of raw and smoothed bycatch rates estimated by the best-fitting single-taxon model in Season 1 (see Table 1 for model). The solid line shows the pattern expected if rates were equal.

1, and 0.004 for Seasons 2 and 4. In the few cells in which the raw rate standard error was smaller, the difference in magnitude was much smaller, never exceeding 0.00004 for Season 1, 0.000022 for Season 2, and 0.0001 for Season 4. This occurred in cells with the some of the highest effort. Since raw rates are more precise in areas of higher effort (Eq. 2), gains in smoothing rates in these cells are negligible. Nevertheless, the goal was to estimate the spatial pattern of bycatch rates across the whole region and the average relative improvement in standard error was 0.000415, 0.00028, and 0.00026 for Seasons 1, 2, and 4, respectively.

Using the model-generated smoothed bycatch rates, we also generated maps to consider the probabilities that the estimated grid cell bycatch rates exceed a particular threshold. We arbitrarily chose 0.0005 marine mammals per 1000 units of effort. There were many areas in which bycatch rates were higher than the threshold selected (Fig. 8). In Season 1, these cells were located in the northern and southern regions of the map. Cells that exceeded the threshold were more scattered in the region in Season 2, while the areas of concern are clustered in the northern area of the map in Season 4.

Cross-taxa analysis

There was positive correlation between bycatch rates of seabirds and marine mammals within grid cells in Seasons 1 and 4 (Table 1). The probability of positive correlation was highest in Season 4 (0.823) indicating there was a similar spatial pattern of bycatch rates between seabirds and marine mammals. A comparison of the mapped smoothed seabird bycatch rates compared with the smoothed marine mammal rates (Fig. 9) illustrates the shared spatial pattern in the northern region of the fished area. Rates were different in the southern region, showing high rates for seabirds and low rates for marine mammals. In contrast, the spatial pattern of bycatch rates between marine mammals and seabirds showed similar high bycatch rates in the southern region during Season 1, while rates in the northern region were low for seabirds and high for marine mammals. The probability of positive correlation was weak in Season 2 (0.368), giving no evidence of a similar spatial pattern of risk between the two taxa.

DISCUSSION

Our results demonstrated that the Bayesian hierarchical spatial model used here addressed inherent limitations of bycatch data and was instrumental in reducing the standard errors in bycatch rates compared with using raw bycatch rates. By applying this method to data from the U.S. Atlantic gill net fishery, we demonstrated a novel approach to mapping bycatch rates that may be used to indicate areas of high bycatch rates, to generate hypotheses about relationships between bycatch and oceanographic variables, and to conduct cross-taxa analyses. Such mapping tools give a
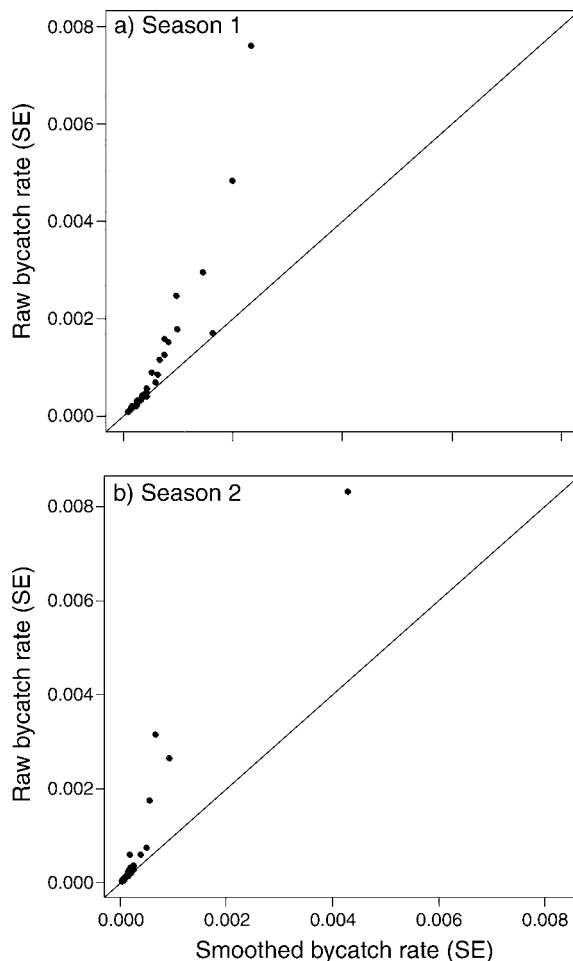

FIG. 4. Comparison of standard errors of raw and smoothed bycatch rates for (a) Season 1 and (b) Season 2. The solid line shows the pattern expected if standard errors were equal.

more comprehensive understanding of spatial patterns of bycatch and provide a tool by which management decisions, such as time-area closures, can be evaluated relative to model-based estimates of bycatch rates that account for variation in fishing effort.

The results of this application illustrate the common problems associated with mapping raw rates and the advantages associated with using Bayesian hierarchical spatial model estimates. Specifically, our Bayesian spatial model addressed the spatial variation in fishing effort and the rarity of bycatch events, and consequently increased the stability of bycatch estimates. The analysis addresses the issue of whether a very high or low raw bycatch rate is an artifact of an area having very low observed fishing effort or whether it reflects the true variability in bycatch rates across a region. As was illustrated by a comparison of raw rates and fishing effort across grid cells, high raw rates were consistently found in areas of low fishing effort (Fig. 1b). This
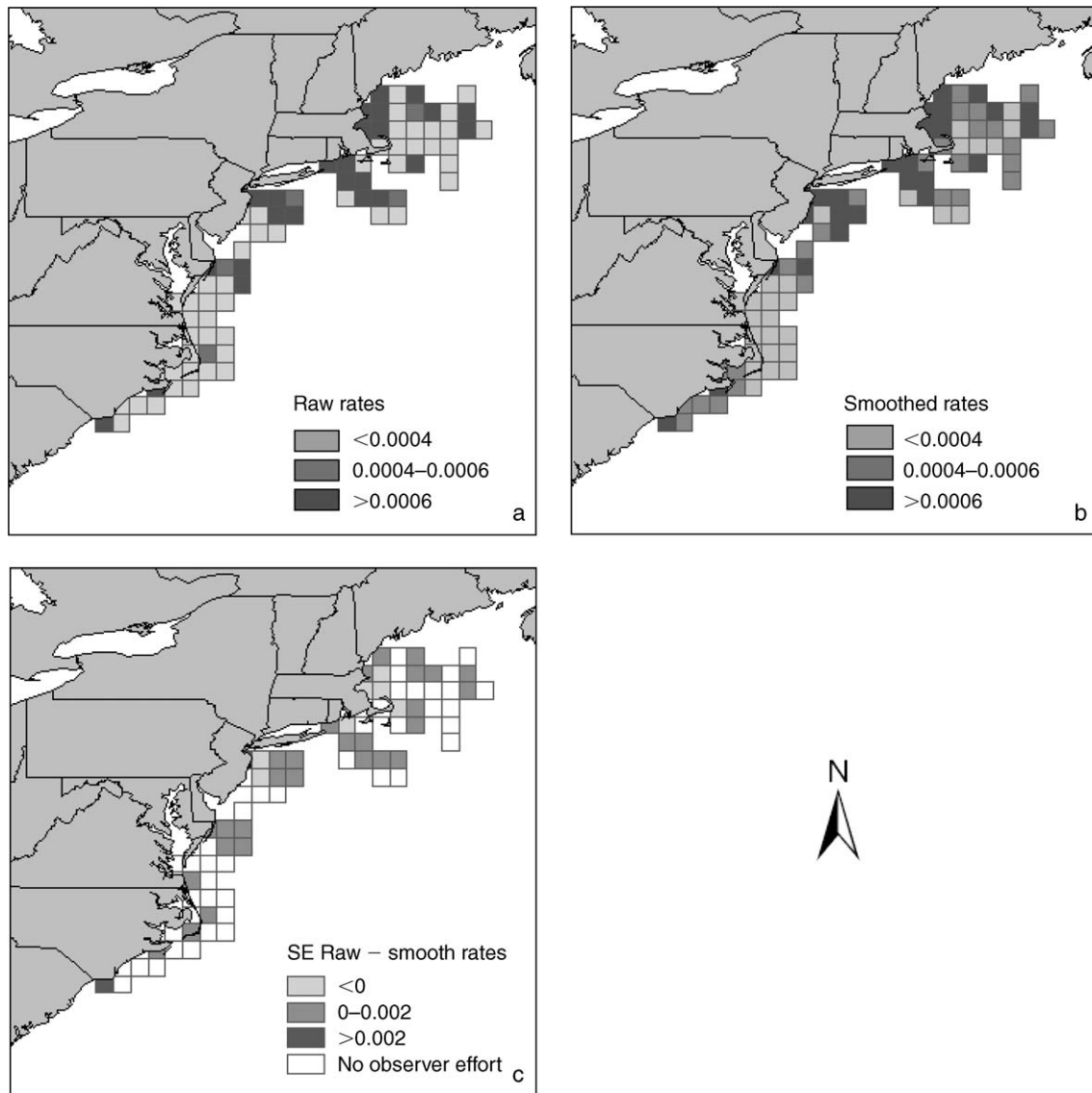
Fig. 5. Marine mammal bycatch rates (number of marine mammals caught per 1000 units of effort) in Season 1: (a) raw bycatch rates, (b) smoothed bycatch rates estimated from best-fit single-taxon model, and (c) the difference in magnitude of the raw rate SEs to the smoothed rate SEs. Positive values indicate areas in which the raw rate SE is larger. Cells with a raw bycatch rate of zero were excluded from the comparison and left blank in the map (see *Results: Single-taxon analysis: Maps*)

highlights the extremely high variability associated with raw rates when low effort is observed and also points to the importance of having high observer coverage and observed effort as higher observer effort is clearly needed to reduce the variability inherent in raw rates. Furthermore, observer programs should be emphasized in low effort regions in contrast to high effort regions in order to reduce variance in the overall estimates. Because areas with low observed fishing effort may yield high bycatch rates, it is possible that management decisions based solely on raw rates may be misleading. Given our findings, there is evidence to suggest that raw bycatch rates need to be adjusted to ensure that they accurately reflect spatial bycatch variability.

A number of other distributions are available to model bycatch data that is over-dispersed relative to the Poisson distribution, such as the zero-inflated Poisson (ZIP) and zero-inflated negative binomial (e.g., Minami et al. 2006). Ver Hoef and Jansen (2007) assumed a zero-inflated Poisson distribution for haul-out counts of harbor seals on glacial ice and modeled spatial patterns using a conditional autoregressive model. We presented an alternative approach for dealing with extra-Poisson variation. The Bayesian hierarchical model described here, which has both a spatial and nonspatial component, can account for the challenges of spatially structured correlation and unstructured overdispersion of bycatch events. This model assumes that there are two
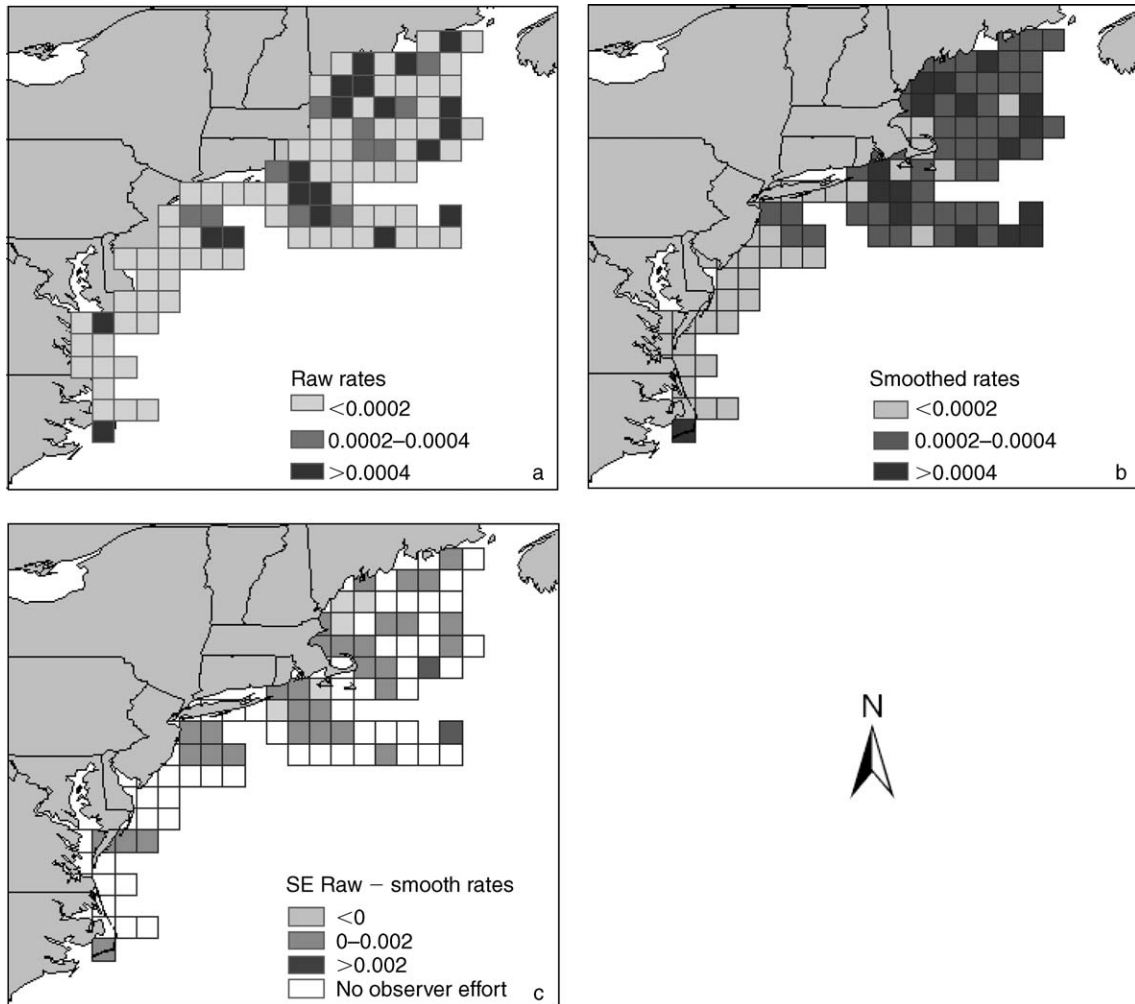
FIG. 6. Marine mammal bycatch rates in Season 2: (a) raw bycatch rates, (b) smoothed bycatch rates estimated from best-fit single-taxon model, and (c) the difference in magnitude of the raw rate SEs to the smoothed rate SEs. Positive values indicate areas in which the raw rate SE is larger. Cells with a raw bycatch rate of zero were excluded from the comparison and left blank in the map (see *Results: Single-taxon analysis: Maps*).

forms of extra variation beyond that governed by the Poisson distribution. First, there is nonspatial over-dispersion arising from having many grid cells with zero counts but also a few with large values (Fig. 1a). The other form of variation is induced by spatial correlation between neighboring grid cells. The ability of the model to distinguish between the two forms of extra-Poisson variation simultaneously allows the degree to which bycatch rates show some form of geographical pattern-ing and the similarity in this pattern between different taxa to be elucidated. This model rests on the assumption that a spatial signal is present in the data and we illustrated the presence spatial correlation prior to fitting the model. If absent, the random effects U_i and S_i are unidentifiable.

Bayesian hierarchical spatial models offer improve-ments in terms of stability of bycatch rate estimates. The

variance reduction of estimates is achieved through borrowing information from neighboring cells. The smoothing procedure results in a trade-off between bias and variance reduction of the bycatch estimates. However, Best et al. (2005) compared the main types of Bayesian hierarchical spatial models available for mapping rates of disease outbreak and found the Besag et al. (1991) model used in this paper performed well. The comparison of estimated standard errors for raw rates and model-based rates illustrate the extent of variance reduction that is achieved using the Besag model here. The Besag model is also flexible in terms of how the spatial areas are defined, which may be a regular or irregular grid (see, for example, Thogmartin et al. 2004). We gave equal weights to all neighbors in the calculation of the spatial random effects. However, non-equal weights can be easily specified. For example, weighting
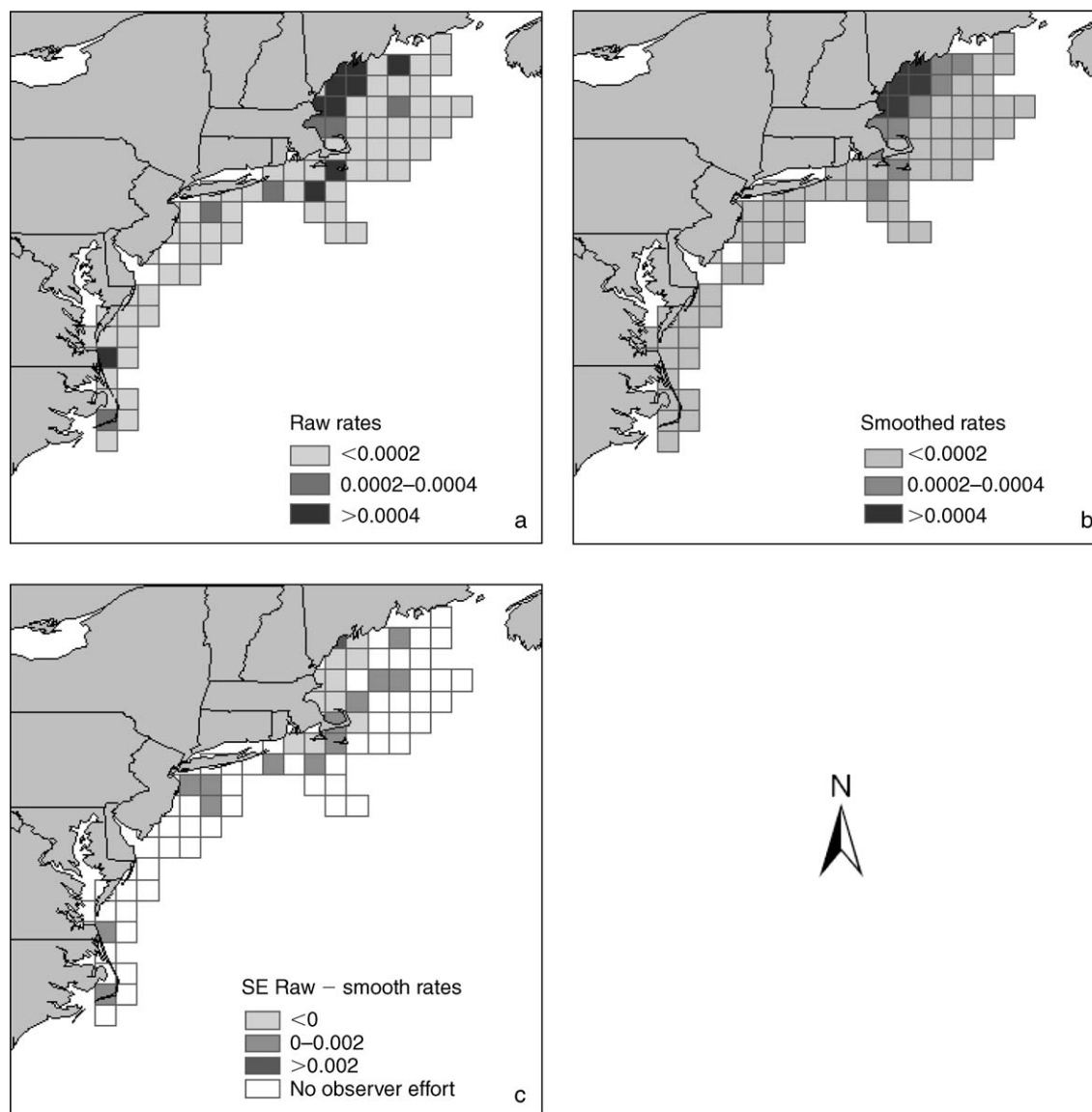
FIG. 7. Marine mammal bycatch rates in Season 4: (a) raw bycatch rates, (b) smoothed bycatch rates estimated from best-fit single-taxon model, and (c) the difference in magnitude of the raw rate SEs to the smoothed rate SEs. Positive values indicate areas in which the raw rate standard error is larger. Cells with a raw bycatch rate of zero were excluded from the comparison and left blank in the map (see *Results: Single-taxon analysis: Maps*).

neighbors by distance between area centroids would be useful if the grid cells were irregular. Thus, these spatial models have the potential for a much broader usage as they can be adjusted for the spatial information at hand. An additional advantage of smoothing bycatch rates is that a more realistic estimate of standard error can be obtained in those areas that had a raw rate of zero.

The Besag model has limitations. Since we defined neighbors for a grid cell as all those sharing a common boundary to that cell, there must be at least one bycatch event in an isolated group of grid cells. A problem encountered with this data set was that due to low observer coverage, rarity of a bycatch event for large

vertebrates, and patchiness of effort, groups of cells arose that all contained zero counts and could not be included in the model. Fitting the model to data from a smaller time scale (e.g., a single year or an individual species) might magnify this problem. To investigate temporal variability, future analyses using this method could instead compare spatial models fit to data from a smaller number of years than the 15 years we used in this study. Alternatively, if we assume the spatial pattern of bycatch remains constant but overall rate fluctuates annually, then a year random effect could be included in the model to capture the year-to-year variability. There are many examples of Bayesian spatiotemporal models
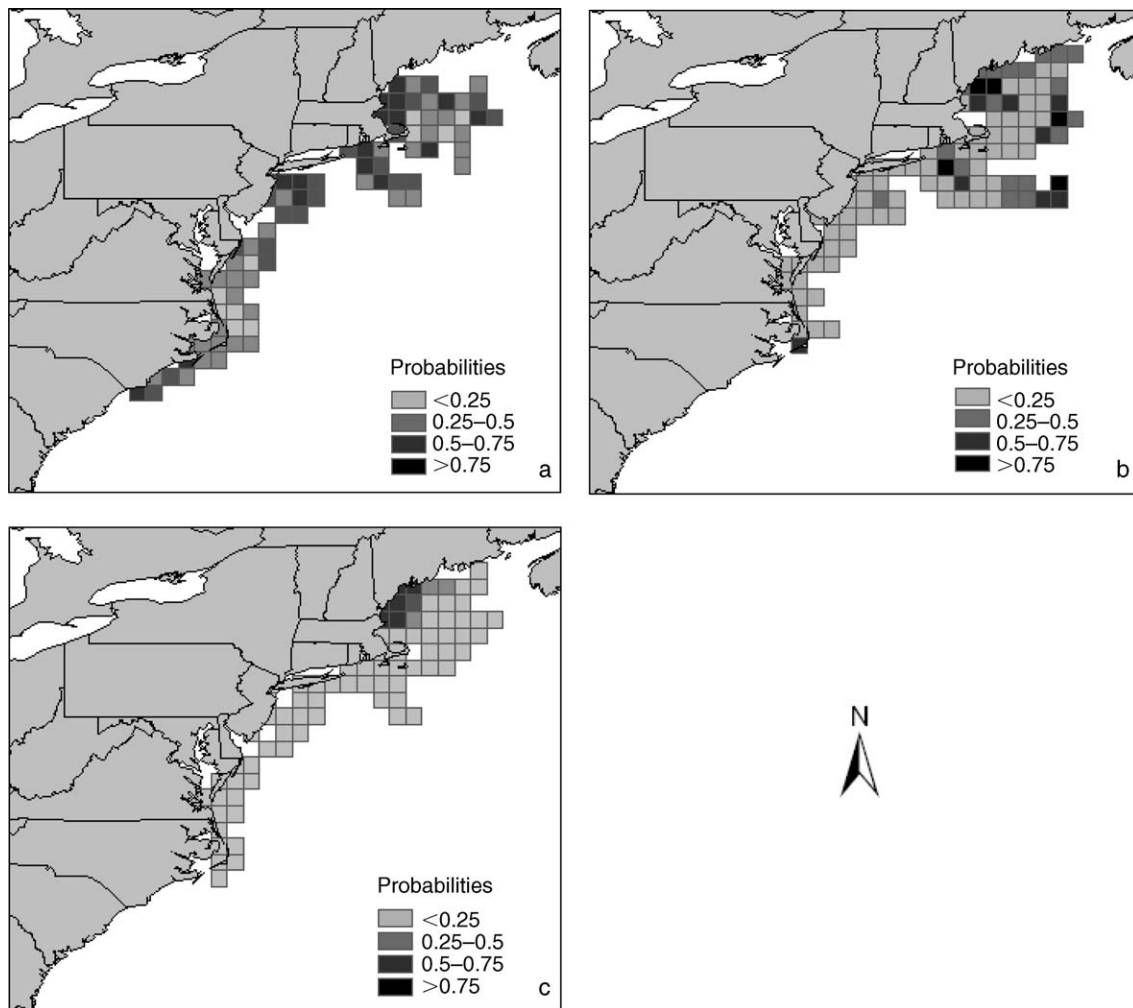
FIG. 8.   Probability that the smoothed bycatch rates of marine mammals are >0.0005 marine mammals per 1000 units of effort in (a) Season 1, (b) Season 2, and (c) Season 4 (see *Results: Single-taxon analysis: Maps*).

fitted to area-referenced data (e.g., Waller et al. 1997, Wikle et al. 1998, Ver Hoef and Jansen 2007). Ver Hoef and Jansen (2007) included a temporal autoregressive model together with a spatial conditional autoregressive model as random effects in a ZIP model. They chose a spatial domain of neighbors for each cell so that the problem of isolated cells with zero counts was avoided. The extent of spatial correlation in our data was not much greater than the width of a grid cell, and therefore expanding the spatial domain of neighbors for a cell beyond those that share a common boundary was not justified in our study.

There are many smoothing procedures available for data referenced by spatial areas (such as presented here) or point locations. For example, Best et al. (2005) consider areal data and compare several Bayesian hierarchical models used to map disease risk. If bycatch were referenced using point locations, then kriging procedures specifically for Poisson or binomially distributed data may be used (Diggle et al. 1998). These

smoothing procedures are also likely to be applicable to bycatch data. However, as the purpose of this paper was to compare the estimated spatial patterns of bycatch rates in a whole region using raw rates vs. those obtained using smoothing models, we focused on a single relevant smoothing technique.

Bayesian hierarchical spatial modeling is an effective and useful tool for exploring geographical distributions of bycatch rates. It has several advantages over traditional mapping of raw rates as well as the added utility of generating maps of bycatch probabilities and facilitating comparison of bycatch patterns across taxa. As illustrated with the U.S. gill net fishery data, one practical application of this spatial modeling approach is the ability to produce maps that highlight the probability that a bycatch rate for a grid cell exceeds some threshold value. These threshold values can reflect management goals relative to the population size or status of a species. Management agencies could then use such maps to identify the most critical management
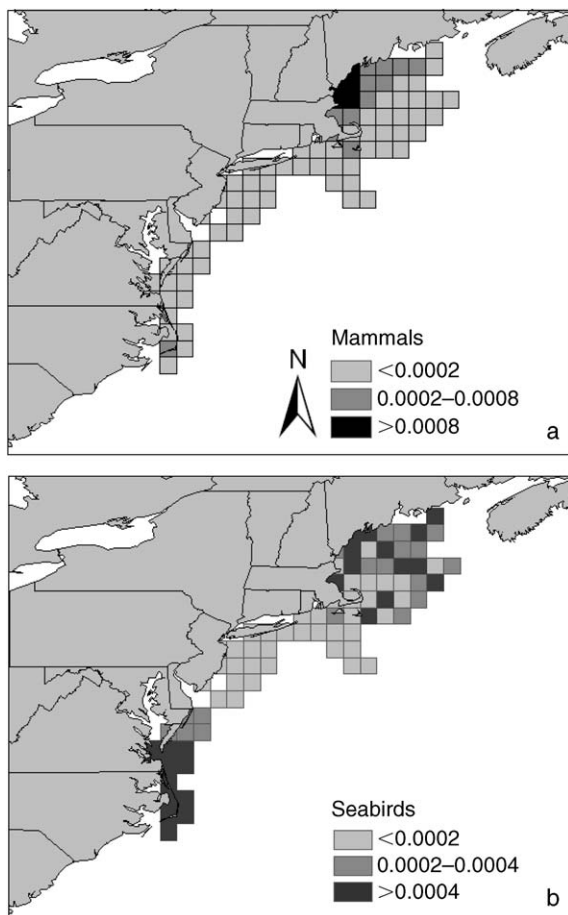
Fig. 9. Comparison of smoothed bycatch rates in Season 4 estimated from the cross-taxa model for (a) marine mammals, and (b) seabirds.

distribution of bycatch, a statistical method that increases the stability of the estimates is critical if management decisions are to be based upon this information.

Recent attempts to manage on an ecosystem-based approach have highlighted the need to conduct multi-taxa analyses and management (Norris et al. 2002). For example, management for one taxon could have detrimental effects on another taxon (Norris et al. 2002, Baum et al. 2003). Here, we demonstrate how this type of model can highlight similarities in spatial patterns of bycatch across taxa. For example, we found evidence of a seasonal positive correlation between the bycatch rates of all marine mammals and seabirds, indicating that the bycatch distribution of both taxa are influenced by some shared spatially structured covariate (i.e., an oceanographic variable) during this season. Such positive correlations may be useful in identifying critical bycatch areas where multiple species across taxa are incidentally captured. A joint mapping analysis can also improve estimates by combining information from multiple taxa across neighboring areas (Best et al. 2005). Finally, the spatial information obtained from the methods outlined here could be used to improve the bycatch rate estimates required in a flexible optimization tool (Leslie et al. 2003). Typically, resource agencies manage for a single species; however, recent attempts to incorporate spatial information on bycatch of multiple taxa have used such a tool to site marine reserves (D'Agrosa 2004). Although an analysis of the ecological mechanisms causing the bycatch patterns was beyond the scope of this paper, future research could integrate model results with the distribution of oceanographic correlates or include the oceanographic covariates into the bycatch model.

Bayesian hierarchical models are an important tool for understanding the true spatial variation in bycatch rates. The advantages of modeling bycatch events to estimate bycatch rates compared with using raw rates are apparent upon comparison of their estimates and corresponding standard errors. This approach can generate alternative summaries of bycatch, such as threshold probabilities, and can be used to conduct multitaxa analyses, both of which have considerable promise for bycatch management and mitigation. Given the success in applying this approach to marine mammals and seabirds bycaught in the U.S. gill net fishery in the northwest Atlantic, these methods have potential for application to other fisheries, and other taxa of conservation concern.

areas. In addition, agencies may be able to use these types of maps post hoc in evaluating time-area closures. For example, the area of high probability of bycatch highlighted in Season 4 in Fig. 8 almost directly overlaps with the midcoast closure that was implemented to reduce harbor porpoise bycatch during that season (U.S. Department of Commerce 1998). Murray et al. (2000) reported that an earlier, smaller closure was too small to have the desired reduction of bycatch. Had a Bayesian hierarchical mapping exercise been conducted a priori, this area could have been identified more precisely. Our post hoc analysis indicates that the current midcoast closure is placed correctly. Further examples of how probability statements generated using Bayesian methods can better communicate results to managers are given in Wade (2000).

One cautionary note regarding the specific example used in our analyses is that U.S. observer data are collected to monitor fishing effort, catch of target species, and bycatch of protected species. Because these data are not collected to expressly understand the spatial

Literature Cited

Baum, J. K., R. A. Myers, D. G. Kehler, B. Worm, S. J. Harley, and P. A. Doherty. 2003. Collapse and conservation of shark populations in the Northwest Atlantic. Science 299:389–392.

Besag, J., J. York, and A. Mollie. 1991. Bayesian image restoration with two applications to spatial statistics. Annals of the Institute of Statistical Mathematics 43:1–21.

Best, N., S. Richardson, and A. Thomson. 2005. A comparison of Bayesian spatial models for disease mapping. Statistical Methods in Medical Research 14:35–39.

Brooks, S. P., and A. Gelman. 1998. General methods for monitoring convergence of iterative simulations. Journal of Computational and Graphical Statistics 7:434–455.

Caretta, J. V., T. Price, D. Petersen, and R. Read. 2005. Estimates of marine mammal, sea turtle, and seabird mortality in the California drift gillnet fishery for swordfish and thresher shark, 1996–2002. Marine Fisheries Review 66: 21–30.

Cressie, N., H. S. Stern, and D. R. Wright. 2000. Mapping rates associated with polygons. Journal of Geographical Systems 2:61–69.

Croxall, J. P., and S. Nicol. 2004. Management of Southern Ocean fisheries: global forces and future sustainability. Antarctic Science 16:569–584.

D'Agrosa, C. E. 2004. The application of spatial analytical techniques toward the conservation of long-lived marine vertebrates: the pelagic longline fishery as a case study. Dissertation. Duke University, Durham, North Carolina, USA.

Diggle, P. J., J. A. Tawn, and R. A. Moyeed. 1998. Model-based geostatistics. Applied Statistics 47:299–350.

Dongchu, S., R. K. Tsutakawa, H. Kim, and Z. He. 2000. Spatial-temporal interaction with disease mapping. Statistics in Medicine 19:2015–2035.

Gelman, A. 2006. Prior distributions for variance parameters in hierarchical models. Bayesian Analysis 1:515–533.

Gelman, A., X.-L. Meng, and H. Stern. 1996. Posterior predictive assessment of model fitness via realized discrepancies. Statistica Sinica 6:733–807.

James, M. C., C. A. Ottensmeyer, and R. A. Myers. 2005. Identification of high-use habitat and threats to leatherback sea turtles in northern waters: new directions for conservation. Ecology Letters 8:195–201.

Kelleher, K. 2005. Discards in the world's marine fisheries. An update. FAO Fisheries Technical paper, No. 470. Rome, Italy.

Knorr-Held, L., and J. Besag. 1998. Modelling risk from a disease in time and space. Statistics in Medicine 17:2045–2060.

Leslie, H., M. Ruckelshaus, I. R. Ball, S. Andelman, and H. P. Possingham. 2003. Using siting algorithms in the design of marine reserve networks. Ecological Applications 13:S185–S198.

Lewison, R. L., L. B. Crowder, A. Read, and S. Freeman. 2004. Understanding impacts of fisheries bycatch on marine megafauna. Trends in Ecology and Evolution 19:598–604.

Leyland, A. H., and C. A. Davies. 2005. Empirical Bayes methods for disease mapping. Statistical Methods in Medical Research 14:17–34.

MacNab, Y. C., and C. B. Dean. 2002. Spatio-temporal modeling of rates for the construction of disease maps. Statistics in Medicine 21:347–358.

Minami, M., C. E. Lennert-Cody, W. Gao, and M. Román-Verdesoto. 2006. Modeling shark bycatch: the zero-inflated negative binomial regression with smoothing. Fisheries Research 84:210–221.

Morgan, B. J. T. 2000. Applied stochastic modelling. Arnold, London, UK.

Murray, K. T., A. J. Read, and A. R. Solow. 2000. The use of time/area closures to reduce by-catches of harbour porpoises: lessons from the Gulf of Maine sink gillnet fishery. Journal of Cetacean Research and Management 2:135–141.

Norris, S., M. Hall, E. Melvin, and J. Parrish. 2002. Thinking like an ocean. Ecological lessons from marine bycatch. Conservation in Practice 3:10–17.

Polovina, J. J., G. H. Balazs, E. A. Howell, D. M. Parker, M. P. Seki, and P. H. Dutton. 2004. Forage and migration habitat of loggerhead (Caretta caretta) and olive ridley (Lepidochelys olivacea) sea turtles in the central North Pacific Ocean. Fisheries Oceanography 13:36–51.

Polovina, J., I. Uchida, G. Balazs, E. A. Howell, D. Parker, and P. Dutton. 2006. The Kuroshio Extension Bifurcation Region: a pelagic hotspot for juvenile loggerhead sea turtles. Deep-Sea Research. Part II—Topical Studies in Oceanography 53:326–339.

Read, A. J., and A. J. Westgate. 1997. Monitoring the movements of harbour porpoises (Phocoena phocoena) with satellite telemetry. Marine Biology 130:315–322.

Ronconi, R. 2007. The spectacular migration of greater shearwaters. Birdwatch Canada 39:4–7.

Spiegelhalter, D. J., N. G. Best, B. P. Carlin, and A. Van der Linde. 2002. Bayesian measures of model complexity and fit (with discussion). Journal of the Royal Statistical Society Series B 64:583–640.

Spiegelhalter, D. J., A. Thomas, N. Best, and W. Gilks. 1996. BUGS 0.5* Bayesian inference under Gibbs sampling manual (version ii). [Computer program.] Medical Research Council Biostatistics Unit, Institute of Public Health, Cambridge University, Cambridge, UK.

Spiegelhalter, D. J., A. Thomas, N. Best, and D. Lunn. 2003. WinBUGS. Version 1.4. Imperial College, London and MRC Biostatistics Unit, Cambridge, UK.

Thogmartin, W. E., J. R. Sauer, and M. G. Knutson. 2004. A hierarchical spatial model of avian abundance with application to Cerulean Warblers. Ecological Applications 14:1766–1779.

Thomas, A., N. Best, D. Lunn, R. Arnold, and D. Spiegelhalter. 2004. GeoBUGS User Manual. Version 1.2. Medical Research Council Biostatistics Unit, Institute of Public Health, Cambridge University, Cambridge, UK.

U.S. Department of Commerce. 1998. Taking of marine mammals incidental to commercial fishing operations; harbor porpoise take reduction plan regulations. Department of Commerce; National Oceanic and Atmospheric Administration. Washington, D.C., USA. Federal Register 63:66464–66490.

Ver Hoef, J. M., and J. K. Jansen. 2007. Space–time zero-inflated count models of harbor seals. Environmetrics 18:697–712.

Wade, P. R. 2000. Bayesian methods in conservation biology. Conservation Biology 14:1308–1316.

Waller, L. A., B. P. Carlin, X. Hong, and A. E. Gelfand. 1997. Hierarchical spatio-temporal mapping of disease rates. Journal of the American Statistical Association 92:607–617.

Wikle, C. K., L. M. Berliner, and N. Cressie. 1998. Hierarchical Bayesian space-time models. Environmental and Ecological Statistics 5:117–154.